

Article

# *In Vitro* and *In Vivo* Evaluation of Titanium Surface Modification for Biological Aging by Electrolytic Reducing Ionic Water

Takahito MIKI <sup>1</sup>, Tomonori MATSUNO <sup>1,\*</sup>, Yoshiya HASHIMOTO <sup>2</sup> , Akiko MIYAKE <sup>3</sup> and Takafumi SATOMI <sup>1</sup>

<sup>1</sup> Department of Oral and Maxillofacial Surgery, The Nippon Dental University School of Life Dentistry at Tokyo, 1-9-20, Fujimi, Chiyoda-ku, Tokyo 102-8159, Japan; miki-t@tky.ndu.ac.jp (T.M.); tsatomi@tky.ndu.ac.jp (T.S.)

<sup>2</sup> Department of Biomaterials, Osaka Dental University, 8-1, Hanazonocho, Kuzuha, Hirakata, Osaka 573-1121, Japan; yoshiya@cc.osaka-dent.ac.jp

<sup>3</sup> Department of Oral Health Engineering, Faculty of Health Sciences, Osaka Dental University, 1-4-4, Makinohonmachi, Hirakata, Osaka 573-1144, Japan; miyake-a@cc.osaka-dent.ac.jp

\* Correspondence: matsunot@tky.ndu.ac.jp; Tel.: +81-3-3261-6558

Received: 21 December 2018; Accepted: 13 February 2019; Published: 19 February 2019



**Abstract:** In this study, using electrolytic reducing ionic water (S-100<sup>®</sup>), a novel surface treatment method safely and easily modifying the surface properties was evaluated *in vitro* and *in vivo*. Ti-6Al-4V disks were washed and the disks were kept standing on a clean bench for one and four weeks for aging. These disks were immersed in S-100<sup>®</sup> (S-100 group), immersed in ultra-pure water (Control group), or irradiated with ultraviolet light (UV group), and surface analysis, cell experiment, and animal experiment were performed using these disks. The titanium surface became hydrophilic in the S-100 group and the amount of protein adsorption and cell adhesion rate were improved *in vitro*. *In vivo*, new bone formation was noted around the disk. These findings suggested that surface treatment with S-100<sup>®</sup> adds bioactivity to the biologically aged titanium surface. We are planning to further investigate it and accumulate evidence for clinical application.

**Keywords:** biological aging; titanium; surface modification

## 1. Introduction

Dental implants are now widely used as a prosthodontic treatment for missing teeth, and products with various surface properties are commercially available. Titanium implants developed early had machined mirror polished surfaces, but it has been clarified that blasted and acid-treated moderately rough surfaces increase protein adsorption and cell adhesion, being advantageous for osseointegration, and these became the current mainstream [1,2].

However, it has recently been reported that biological aging, representing decreases in hydrophilicity and protein adsorption due to adherence of carbon and nitrogen in the air to the titanium implant surface with time, influences osseointegration [3]. This is caused by a decrease in hydrophilicity and changes in the surface electrical potential due to reduced surface energy by adherence with carbohydrates in the air to the titanium surface. It has been reported that as the surface becomes hydrophobic, adsorption of blood adhesion protein, such as fibronectin, significantly decreases compared with adsorption to the hydrophilic surface [4], and this is considered to influence the bone-implant contact ratio (BIC) at an early stage of the implant placement [5–7]. This hydrophilicity of the titanium surface is evaluated based on the contact angle, and a surface with a contact angle smaller than 60° and 5° or smaller are regarded as hydrophilic and superhydrophilic, respectively [3].

It has also been reported that the speed of change to hydrophobic increases as the surface roughness increases [4]. Furthermore, electrical polarity decreases on hydrophobic metal surfaces, to which positively charged ions, such as  $\text{Ca}^{2+}$ , and negatively charged cells do not readily adhere [1,8,9].

Against this biological aging of the titanium surface, various countermeasures have recently been taken. The photofunctionalization technique, modifying the titanium surface to make it superhydrophilic by ultraviolet (UV) irradiation [3], and a method to prevent exposure to the air by enclosing implants in saline at the time of factory shipment [10] have been investigated, developed, and clinically used. In photofunctionalization, carbohydrates adhered to the titanium surface are degraded by reactive oxygen generated by UV irradiation and the surface property is changed to superhydrophilic. As a result, elevation of the maximum value of BIC to nearly 100% from the normal value,  $45\% \pm 16\%$  or 50%–75%, has been reported [1,5].

On the other hand, we have developed and reported an original technique in which aged Ti-6Al-4V disks were immersed in 3%  $\text{H}_2\text{O}_2$  and treated with hydrothermal oxidation at  $121^\circ\text{C}$  /0.2 MPa for 20 min using an autoclave to form a new titanium oxide layer with an about 90 nm thickness, changing the titanium surface to hydrophilic [11]. Using this method, a hydrophilic titanium surface was acquired and protein adsorption and cell adhesion increased. However, this method had the disadvantage that it changes the original titanium surface microstructure.

In this study, to safely and easily improve biological aging, we focused on electrolytic reducing ionic water (S-100<sup>®</sup>) [12]. S-100<sup>®</sup> is special functional water containing abundant  $\text{OH}^-$  ions and it removes/cleans off adhering substances by inducing an electrical repulsion force between the adhering substance and matrix. Therefore, in this study, we investigated whether surface treatment by S-100<sup>®</sup> can easily remove pollutants such as carbon, which cause biological aging without changing the surface structure of titanium.

## 2. Materials and Methods

### 2.1. Titanium Disk Treatment

For the titanium disk (Ti disk), mirror-polished Ti-6Al-4V disks with a 9.5 mm diameter and 1.0 mm thickness (Osaka Yakken, Osaka, Japan) were used. For pre-treatment, Ti disks were immersed in ethanol, acetone, and double distilled water (DDW) and cleaned by ultrasonication for 10 min. We defined the disk immediately after pre-treatment as “fresh”. Then, the disks were kept standing on a clean bench for 1 and 4 weeks, followed by immersion for 3 min in S-100<sup>®</sup> (A. I. System Products, Aichi, Japan) or DDW or irradiated with UV light using a 15 W germicidal lamp ( $\lambda = 253.7$  nm, National, Osaka, Japan) for 48 h on the clean bench designated as Control, S-100, and UV groups, respectively.

### 2.2. Trace Element Analysis

As the chemical composition of fresh and four-week aged Ti disk in the Control and S-100 groups, trace elements were measured by wide (1300.00–0.00 eV, 20.000 s) and narrow (C1s: 298.00–278.00 eV, N1s: 411.00–391.00 eV, O1s: 543.00–523.00 eV, Ti2p: 469.00–449.00 eV, 20.000 s) scanning of X-ray photoelectron spectroscopy (XPS) (PHI-X Tool, ULVAC-PHI, Kanagawa, Japan) ( $n = 4$ ).

### 2.3. Evaluation of Hydrophilicity

First, 0.5  $\mu\text{L}$  of DDW was dripped on the fresh and one-week or four-week aged Ti disk surface. Then, the contact angle was measured using a contact angle gauge (LSE-ME3, Nick, Saitama, Japan) to evaluate hydrophilicity ( $n = 5$ ).

### 2.4. Protein Adsorption Test

On the fresh and four-week aged Ti disk surfaces of the Control, S-100, and UV groups, 200  $\mu\text{L}$  of 1.0 mg/mL bovine serum fibronectin was dripped and protein adsorption was measured after 24 h using a protein assay kit (Bio-Rad protein assay kit, Bio-Rad Laboratories, Hercules, CA, USA).

### 2.5. Cell Culture

An osteoblast-like cell line, MC3T3E-1 (Riken cell bank, Tsukuba, Japan), was cultured in  $\alpha$ -MEM (Nakarai, Kyoto, Japan) containing 10% fetal bovine serum (Biowest, Nuaille, France) and 1% penicillin-streptomycin (Life Technologies, Tokyo, Japan) at 37 °C in 5% CO<sub>2</sub>. The culture medium was exchanged every 3 days.

### 2.6. Cell Adhesion Test

On the fresh and four-week aged Ti disks of the Control, S-100, and UV groups placed in a 24 well plate, 500  $\mu$ L of MC3T3-E1 cells was seeded ( $4.0 \times 10^4$  cells/well). After incubation for 24 h, the cells were stained with rhodamine-phalloidin (Wako Pure Chemical, Osaka, Japan) and 4',6-diamidino-2-phenylindole (DAPI, Nakarai, Kyoto, Japan) and observed under a confocal laser microscope (LSM700, ZEISS, Tokyo, Japan). The area adhered to by stained cells was quantitated using image analysis software (ImageJ, NIH, Bethesda, ML, USA).

### 2.7. Cell Proliferation Test

Cells were seeded on the fresh Ti disk surface under the same conditions as those of the cell adhesion test and cell proliferation was measured after incubation for 24 and 72 h. CellTiter96<sup>®</sup> (Promega KK, Madison, WI, USA) was added to the 24 well plates, the plates were incubated at 37°C for 15 min to develop color, and the absorbance was measured at 490 nm wavelength using a microplate reader (Bio-Rad Model 680, Bio-Rad Laboratories, Hercules, CA, USA).

### 2.8. Animal Experiment

All animal experiments were performed in accordance with the Guidelines for the Care and Use of Laboratory Animals under the approval of the Animal Care Committee of the School of Life Dentistry, Nippon Dental University (approval numbers 17–16). The combination of three anesthetics (butorphanol tartrate, medetomidine hydrochloride, and midazolam) was intramuscularly injected into the thigh of six New Zealand white rabbits for general anesthesia. After disinfecting the bilateral thighs with povidone iodine, local anesthesia with 2% Xylocaine was administered. A skin incision was made using a #15 scalpel, the muscle layer was dissected, and the periosteum was incised to expose the femur. A groove with a 10.0 mm length, 1.0 mm width, and 10.0 mm depth was prepared in the femur using an ultrasonic bone cutting machine (PIEZOSURGERY, Carasco, Italy) (Figure 1a). A four-week aged Ti disk immersed in saline or S-100<sup>®</sup> for 3 min was placed in the groove (Figure 1b). The wound was closed by suturing the periosteum with 5-0 VICRIL<sup>®</sup> and skin with 5-0 nylon. At 4 weeks after placement, the rabbits were euthanized by overdosing pentobarbital sodium through the auricular vein and the femur was excised. After micro computed tomography (CT) non-decalcified samples were prepared from the excised femur and subjected to Villanueva bone staining. BIC within a 5-mm range from the center to the bone marrow side of the disk was determined (Figure 2). BIC was calculated by dividing the length of direct contact between the bone and disk by the disk circumference using ImageJ.

(BIC = Length of bone contact to the Ti disc surface/Length of the Ti disc surface)

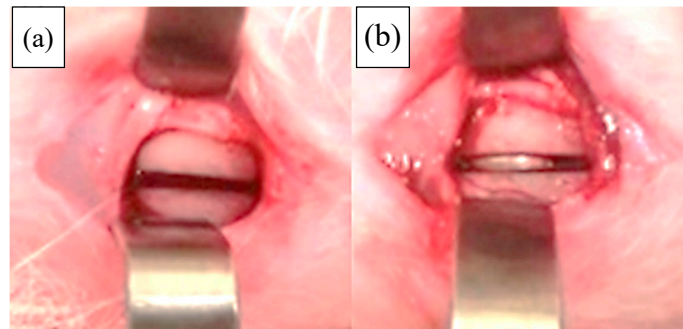


**Figure 1.** Ti disk placement in the rabbit femur. (a) Groove preparation for Ti disk placement, (b) after Ti disk placement.

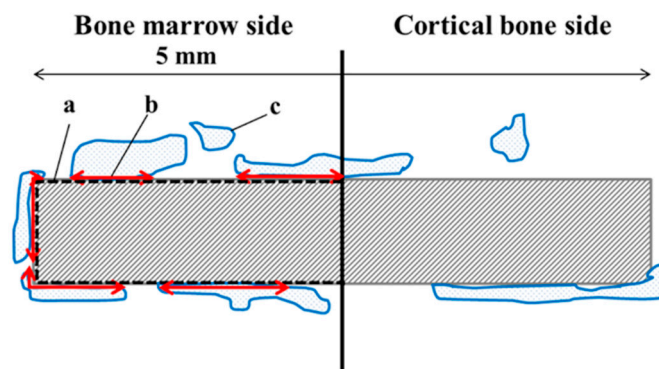


**Figure 2.** Schema of bone–implant contact (BIC) measurement range. (a) Length of the Ti disk surface (black dotted line), (b) length of bone contact to the Ti disk surface (red arrow), and (c) new bone (blue line area).

### 2.9. Statistical Analysis

The *in vitro* results were analyzed using one way layout analysis of variance followed by Tukey's test. The *in vivo* results were analyzed using the t-test.

## 3. Results

### 3.1. Trace Element Analysis

In wide measurement, C, O, and Ti were detected in both Control and S-100 groups. C decreased and O increased in the S-100 group (Figure 3a). In narrow measurement, C decreased and O increased in the C1s, O1s, N1s, and Ti2p measurement items in the S-100 group (Figure 3b).

### 3.2. Changes in Contact Angle Measurement

DDW dripped on the Ti disk was dome-shaped in the Control group, but it spread widely over the Ti disk surface in the S-100 and UV groups, showing favorable wettability (Figure 4). The contact angle increased with time in all groups and a significant difference was noted between the fresh and one-week aged disks and between the fresh and four-week aged disks in the Control group. In addition, the value was significantly smaller in the S-100 and UV groups than in the Control group at all measurement time-points. On comparison between the S-100 and UV groups, the value was significantly smaller in the UV group at fresh and 1 week, but no significant difference was noted at 4 weeks (Figure 5).

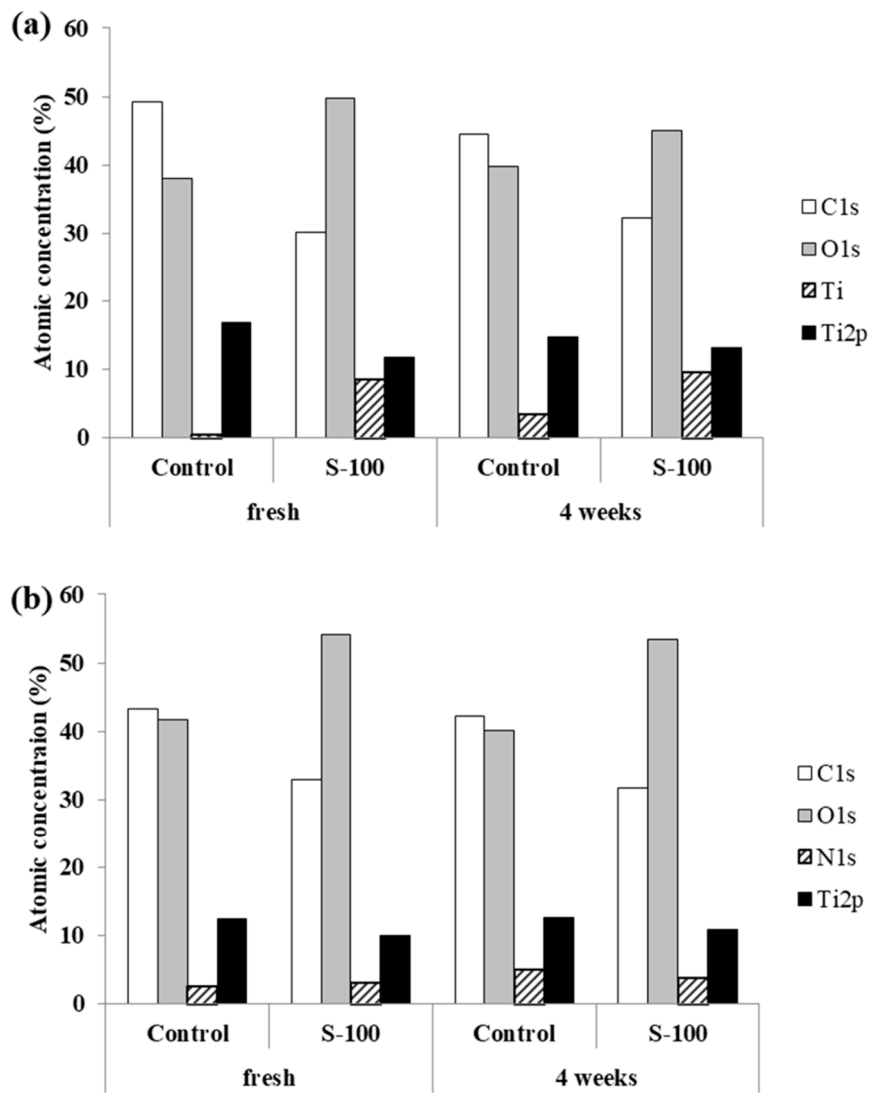


**Figure 3.** Trace element analysis (X-ray photoelectron spectroscopy (XPS)): (a) wide scan, (b) narrow scan (n = 4).

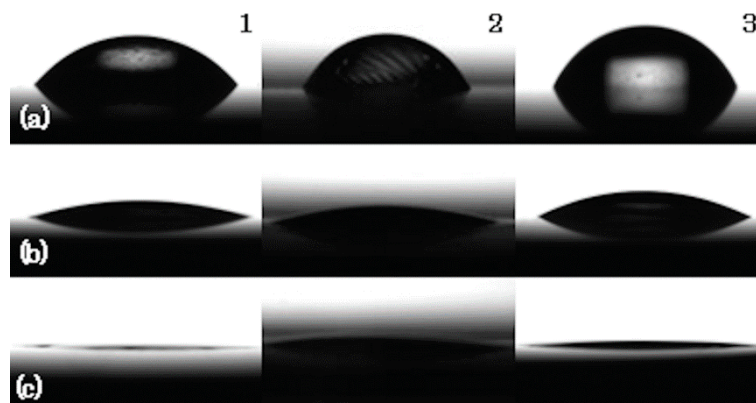


**Figure 4.** Photographs of contact angle measurement. (a) Control, (b) S-100, and (c) UV. 1: fresh, 2: 1 week, 3: 4 weeks.

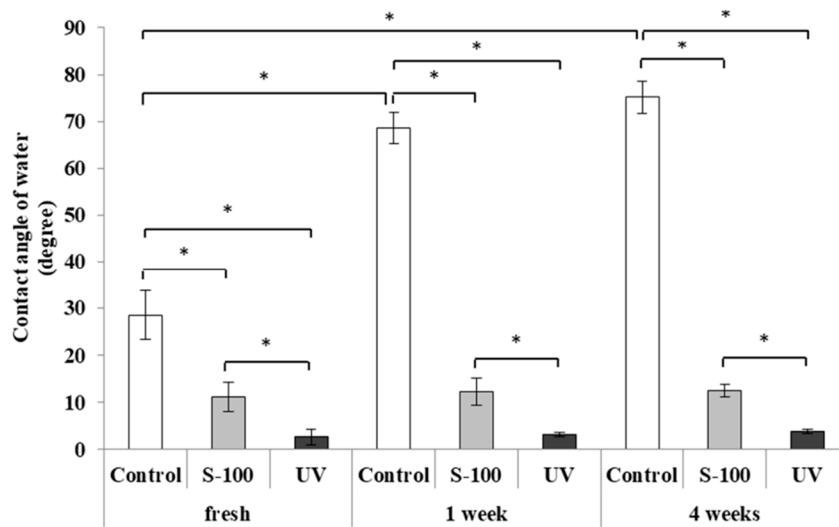


Figure 5. Contact angle (\*  $p < 0.01$ , Tukey test,  $n = 5$ ).

### 3.3. Protein Adsorption

The value was significantly higher in the UV group than in the Control group at fresh, but no significant difference was noted between the UV and S-100 groups. At 4 weeks, the value was significantly higher in the S-100 and UV groups than in the Control group (Figure 6).

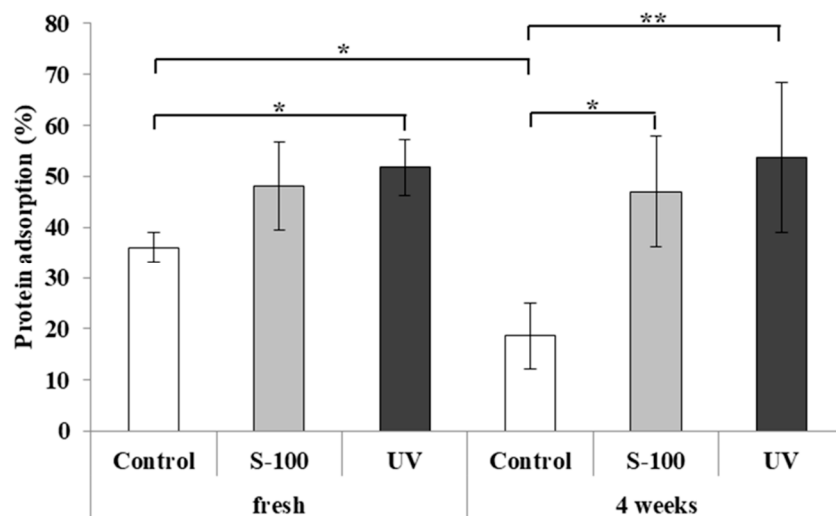
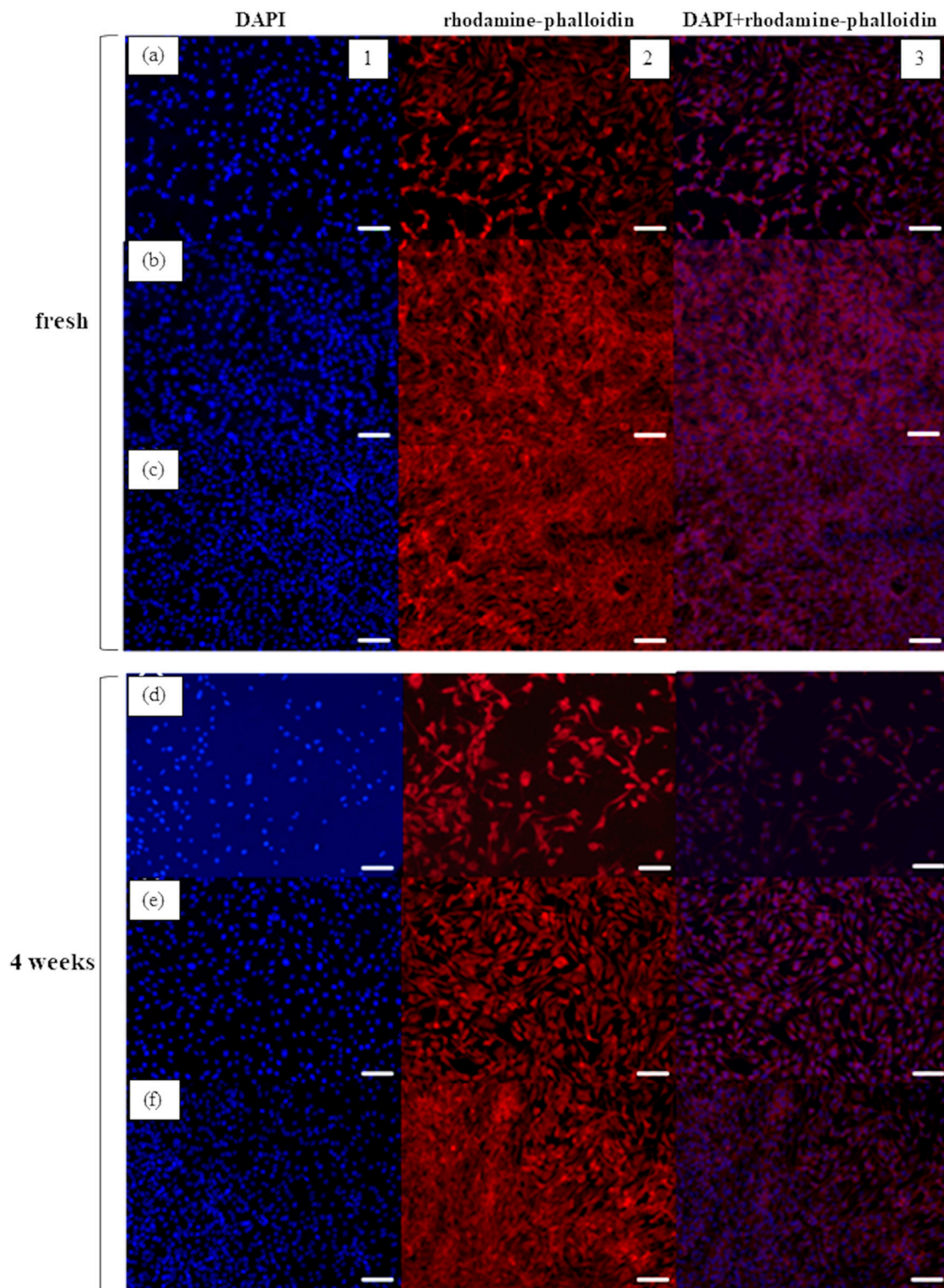


Figure 6. Protein adsorption test (\*  $p < 0.05$ , \*\*  $p < 0.01$ ,  $n = 5$ ).

### 3.4. Cell Adhesion

MC3T3-E1 cells extending cell processes on all over the Ti disk was noted in the S-100 group (Figure 7). The cell attachment area was significantly larger in the UV group than in the Control and S-100 groups at fresh, whereas it was significantly larger in the S-100 and UV groups than in the Control group at 4 weeks (Figure 8).



**Figure 7.** Cell adhesion (x10), 4',6-diamidino-2-phenylindole (DAPI) rhodamine staining. (a) Control/fresh, (b) S-100/fresh, (c) UV/fresh, (d) Control/4 weeks, (e) S-100/4 weeks, (f) UV/4 weeks. 1: DAPI, 2: rhodamine-phalloidin, 3: DAPI + rhodamine-phalloidin (scale bar = 100  $\mu$ m).

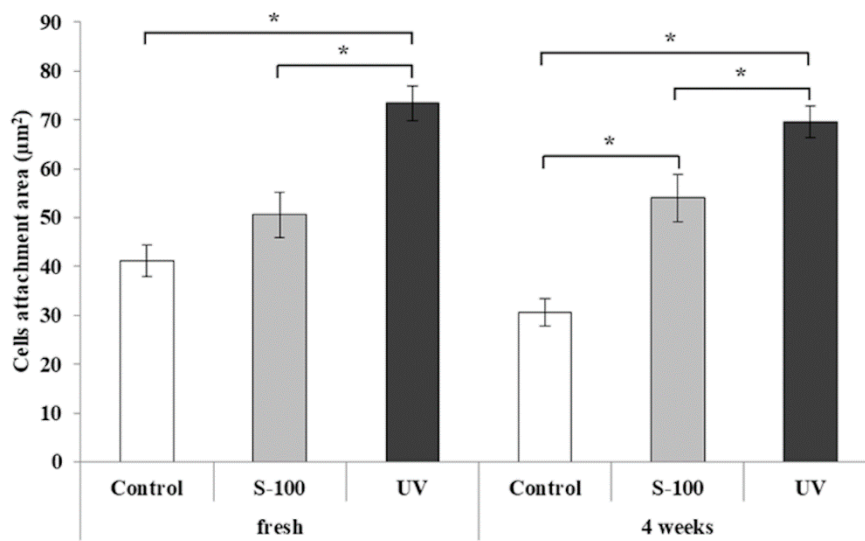


Figure 8. Cell attachment area (\*  $p < 0.01$ , Tukey test,  $n = 5$ ).

### 3.5. Cell Proliferation

At 24 h, the proliferation ability was significantly higher in the S-100 and UV groups than in the Control group. At 72 h, the ability was significantly higher in the UV group than in the Control and S-100 groups (Figure 9).

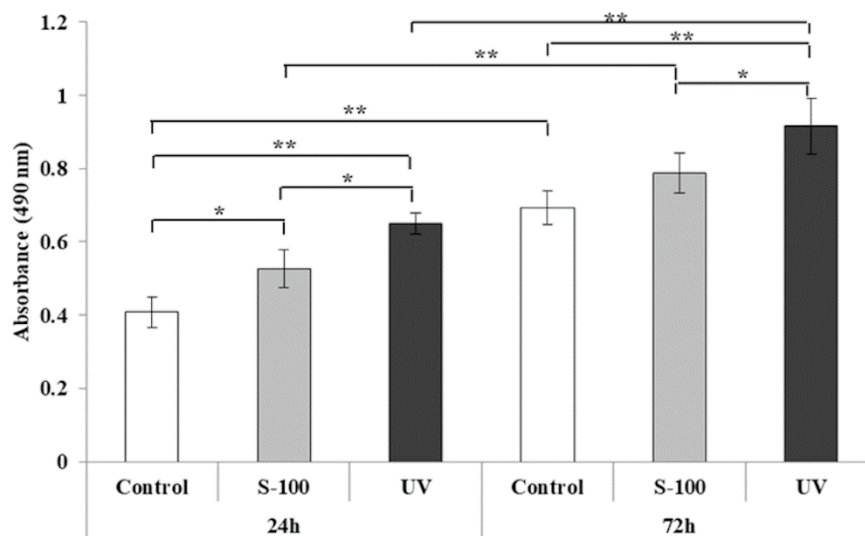
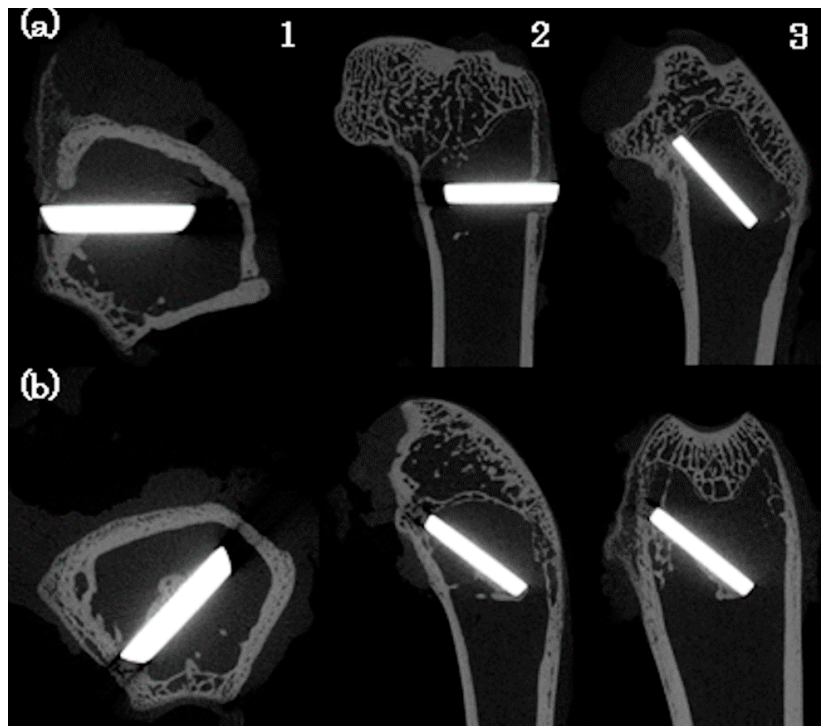


Figure 9. Cell proliferation (\*  $p < 0.05$ , \*\*  $p < 0.01$ , Tukey test,  $n = 5$ ).

### 3.6. Animal Experiment

On micro CT, active new bone formation was noted around the Ti disk on the bone marrow side in the S-100 group compared with that in the Control group (Figure 10). On Villanueva bone staining, many osteoid fragments stained red purple were noted on the bone marrow side of the disk in the S-100 group compared with that in the Control group (Figure 11). In addition, the BIC value was significantly higher in the S-100 group than in the Control group (Figure 12).



**Figure 10.** Micro CT of rabbit femur. (a) Control, (b) S-100. 1: X–Y plane, 2: Y–Z plane, 3: Z–X plane.

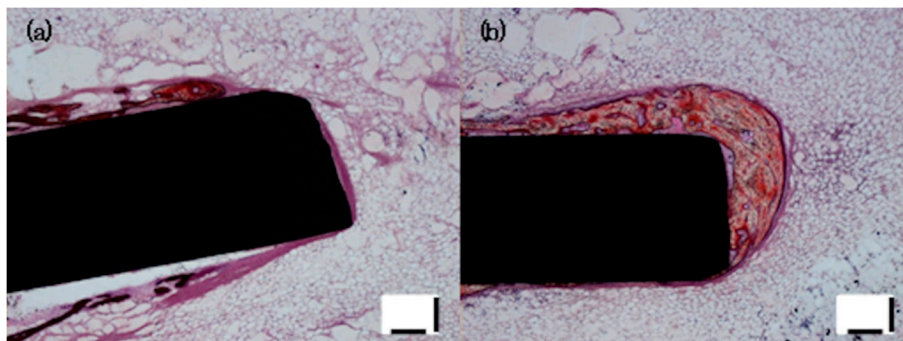


**Figure 11.** Histological evaluation (Villanueva bone staining, x4). (a) Control, (b) S-100 (scale bar = 100  $\mu$ m).

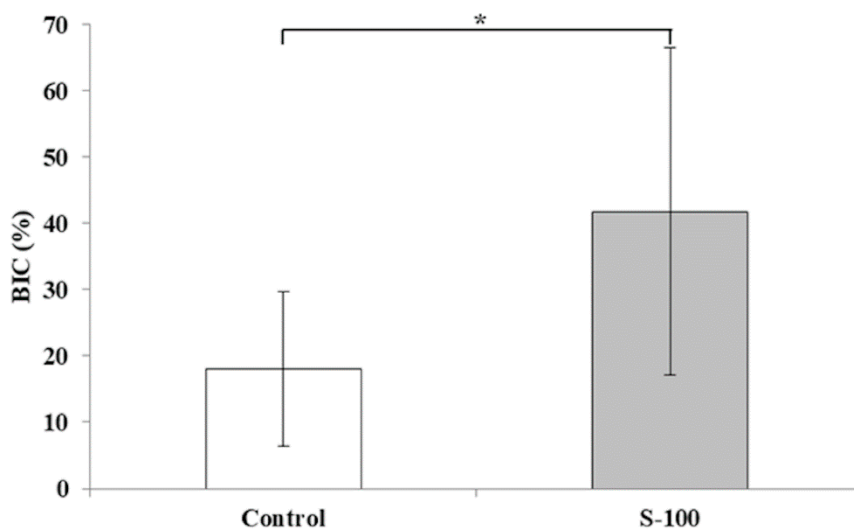


**Figure 12.** Animal experiment; BIC (\*  $p < 0.05$ ,  $t$ -test,  $n = 5$ ).

#### 4. Discussion

It is considered that the implant surface properties affect behaviors of cells and proteins necessary to acquire osseointegration, and biological aging of titanium has been clarified to decrease protein adsorption and cell adhesion to the Ti surface [1,4,13]. On this basis, surface modification, such as photofunctionalization, is performed and the implant surface made hydrophobic by biological aging is cleaned and returned to hydrophilic [5]. Recently, commercial implants have been given an original surface morphology of each company, and in some products, fixture is stored in saline to block exposure to the air to prevent biological aging [10]. Although this photofunctionalization may be effective to prevent biological aging of titanium, there are several problems, such as the fact that the UV is expensive dedicated equipment and long operation times are necessary.

Thus, we designed and evaluated a new treatment method capable of modifying the surface easily within a short time using no special equipment even in a general dental clinic. S-100<sup>®</sup> used in this study is special functional water containing abundant OH<sup>-</sup> ions [12], which detach/clean off adhering substances by inducing an electrical repulsion force between the adhering substances and matrix. We considered that the surface can be cleaned and modified utilizing this action.

Regarding the aging of titanium, it has been clarified that trace elements in the air, such as carbon, adhere to the titanium surface and decrease the surface polarity, and the surface becomes hydrophobic as the surface energy decreases [3,9]. The percentage of carbon differed between the Control and S-100 groups on trace element analysis, suggesting that acquisition of hydrophilicity by treatment with S-100<sup>®</sup> was associated with removal of carbon and the increase in oxygen was the result of exposure of the titanium oxide layer of the titanium surface by removal of carbon.

The titanium implant surface is hydrophilic and having polarity immediately after processing and adhesion protein can bind to it directly or via Ca<sup>2+</sup> [3,13], but polarity is lost as carbohydrates in the air adhere to the titanium surface and the contact angle increases to 60° or greater, with which the surface becomes hydrophobic and protein adsorption decreases. When photofunctionalization was applied to the surface, the contact angle decreased to below 5°, being superhydrophilic [3]. In our study, the results of contact angle measurement performed as evaluation of hydrophilicity clarified that S-100 treatment decreased the contact angle and the surface was changed from hydrophobic to hydrophilic. However, the S-100 treatment could not improve superhydrophilicity such as the UV treatment. This may have been because of the fact that introduction of the hydroxyl groups to the titanium surface by the photocatalytic effect was combined in the principle of acquisition of superhydrophilicity by photofunctionalization, in addition to degradation of carbohydrates by reactive oxygen [14,15]. However, in our preliminary experiment in which the sandblasted surface was treated with S-100<sup>®</sup>, the contact angle decreased to below 5°, acquiring superhydrophilicity.

On the protein adsorption test, a significant difference was noted between fresh and 4 weeks in the Control group, clarifying that protein adsorption decreased as a result of aging-associated hydrophobicity of the surface at 4 weeks compared with that at fresh. In addition, no significant difference was noted between the Control and S-100 groups at fresh, but the surface changed to hydrophobic in the Control group at 4 weeks after progression of aging and the amount of protein adsorption was higher in the S-100 and UV groups with a hydrophilic surface. It was also suggested that because the hydroxyl group mediates protein binding in adsorption to the titanium surface [16], while hydrophilicity was acquired through removal of carbohydrates in the S-100 group, in the UV group, photofunctionalization not only degraded carbohydrates, but also introduced the hydroxyl group into the surface, resulting in a higher amount of adsorption than that in the S-100 group.

On the cell adhesion test, the cell attachment area was significantly larger in the UV group than in the Control and S-100 groups at fresh and in the S-100 and UV groups than in the Control group at 4 weeks. It has been reported that cell adhesion decreases on the surface with aging-associated hydrophobicity and influences the subsequent cell response and contributes to proliferation and differentiation of osteoblasts [16,17]. In our study, carbon adhered to and decreased the surface energy in the Control group and changes in the surface electrical potential made cells unable to readily adhere

to the titanium surface, whereas many cells adhered in the S-100 and UV groups, which may have been because of an increase in the surface energy due to removal of carbon and changes in the surface electrical potential. On rhodamine–phalloidin staining, the cellular skeleton was thin and a space was present between cells in the Control group, whereas the cellular skeleton was thick and cells densely proliferated in the S-100 group and cells were more densely present in the UV group.

On the cell proliferation test, the value was significantly higher in the S-100 and UV groups than in the Control group at 24 h and significantly higher in the UV group than in the Control and S-100 groups at 72 h. On the basis of the fact that surface hydrophilicity contributes to early cell adhesion [17], the value may have been high in the S-100 and UV groups to which hydrophilicity was added at 24 h, and the value was higher in the UV group with superhydrophilicity at 72 h.

On the animal experiment, BIC was significantly higher in the S-100 group than in the Control group. It has been reported that hydrophilicity of the titanium surface is involved in adsorption of various proteins and cytokines influencing osseointegration and cell adhesion, decreasing BIC [18–21], which may have been associated with the higher BIC value in the hydrophilic S-100 group than that in the hydrophobic Control group. Active new bone formation was observed around the Ti disk in the S-100 group compared with that in the Control group. To acquire sufficient osseointegration of implant surface, appropriate bone quality, fixture microstructure, and bone bioactivity are important [22–25]. In this study, mirror-polished titanium discs were placed in insufficient areas of cancellous bone. Thus, the BIC of the S-100 treatment was twice as high as the control—its value was about 40%. However, if micro rough surface titanium disks were used, the BIC will be further increased.

In addition, it has been reported that UV treated titanium surface showed significantly higher BIC in vivo study [3,21]. In this in vitro study, UV treatment showed significantly higher bioactivity than the S-100 treatment. Even though UV treated disks were used for in vivo study, the BIC of UV treated disk was considered to be significantly higher than the S-100 treatment. Furthermore, given the reduction in the number of animals, UV treated titanium disks were not used in this in vivo study.

For implant surface treatment, installment of special equipment in a disinfection room of the dental clinic is necessary [26]. The results of the in vitro tests clarified that surface activity almost equivalent to that acquired by photofunctionalization was acquired by short-time S-100 treatment. In addition, the in vivo test shows that biological aging improves and promotes new bone formation. These results suggest that this treatment method functionalizes the Ti surface at chair-side easily at a low cost with space-saving. We are planning to perform mechanical and histological investigations in vivo to accumulate evidence aiming at clinical application.

## 5. Conclusions

A new titanium surface modification method using special electrolytic reducing ionic water containing abundant OH<sup>−</sup> ions was investigated and its usefulness as a low-cost simple surface treatment method was indicated. It was suggested that application of this treatment immediately before the use of implant placement promotes osseointegration at an early stage, shortening the healing period.

**Author Contributions:** T.M. (Tomonori MATSUNO) and T.M. (Takahito MIKI) conceived and designed the experiments; T.M. (Tomonori MATSUNO) and T.M. (Takahito MIKI) performed the experiments; Y.H., T.M. (Takahito MIKI), and A.M. analyzed the data; T.M. (Tomonori MATSUNO), T.M. (Takahito MIKI), Y.H., and A.M. contributed reagents/materials/analysis tools; T.S., T.M. (Takahito MIKI), and T.M. (Tomonori MATSUNO) wrote the paper.

**Funding:** This work was supported by JSPS KAKENHI Grant Number 15K11227.

**Conflicts of Interest:** The authors declare no conflict of interest.

## References

1. Jemat, A.; Ghazali, M.J.; Razali, M.; Otsuka, Y. Surface modifications and their effects on titanium dental implants. *BioMed. Res. Int.* **2015**, *2015*, 791725. [[CrossRef](#)] [[PubMed](#)]

2. Smeets, R.; Stadlinger, B.; Schwarz, F.; Beck-Broichsitter, B.; Jung, O.; Precht, C.; Kloss, F.; Gröbe, A.; Heiland, M.; Ebker, T. Impact of dental implant surface modifications on osseointegration. *BioMed. Res. Int.* **2016**, *201*, 6285620. [[CrossRef](#)] [[PubMed](#)]
3. Att, W.; Hori, N.; Takeuchi, M.; Ouyang, J.; Yang, Y.; Anpo, M.; Ogawa, T. Time-dependent degradation of titanium osteoconductivity: An implication of biological aging of implant materials. *Biomaterials* **2009**, *30*, 5352–5363. [[CrossRef](#)] [[PubMed](#)]
4. Hori, N.; Att, W.; Ueno, T.; Sato, N.; Yamada, M.; Saruwatari, L.; Suzuki, T.; Ogawa, T. Age-dependent degradation of the protein adsorption capacity of titanium. *J. Dent. Res.* **2009**, *88*, 663–667. [[CrossRef](#)] [[PubMed](#)]
5. Aita, H.; Hori, N.; Takeuchi, M.; Suzuki, T.; Yamada, M.; Anpo, M.; Ogawa, T. The effect of ultraviolet functionalization of titanium on integration with bone. *Biomaterials* **2009**, *30*, 1015–1025. [[CrossRef](#)]
6. García, A.J.; Ducheyne, P.; Boettiger, D. Effect of surface reaction stage on fibronectin-mediated adhesion of osteoblast-like cells to bioactive glass. *J. Biomed. Mater. Res.* **1998**, *40*, 48–56. [[CrossRef](#)]
7. Hirota, M.; Tanaka, M.; Ishijima, M.; Iwasaki, C.; Park, W.; Ogawa, T. Effect of photofunctionalization on ti6al4v screw stability placed in segmental bone defects in rat femurs. *J. Oral Maxillofac. Surg.* **2016**, *74*, 861.e1–861.e16. [[CrossRef](#)]
8. Kohavi, D.; Badihi Hauslich, L.; Rosen, G.; Steinberg, D.; Sela, M.N. Wettability versus electrostatic forces in fibronectin and albumin adsorption to titanium surfaces. *Clin. Oral Implants Res.* **2013**, *24*, 1002–1008. [[CrossRef](#)]
9. Zhou, Z.; Li, W.; He, T.; Qian, L.; Tan, G.; Ning, C. Polarization of an electroactive functional film on titanium for inducing osteogenic differentiation. *Sci. Rep.* **2016**, *6*, 35512. [[CrossRef](#)]
10. Schwarz, F.; Herten, M.; Sager, M.; Wieland, M.; Dard, M.; Becker, J. Bone regeneration in dehiscence-type defects at chemically modified (SLActive<sup>®</sup>) and conventional sla titanium implants: A pilot study in dogs. *J. Clin. Periodontol.* **2007**, *34*, 78–86. [[CrossRef](#)]
11. Yoneyama, Y.; Matsuno, T.; Hashimoto, Y.; Satoh, T. In vitro evaluation of h2o2 hydrothermal treatment of aged titanium surface to enhance biofunctional activity. *Dent. Mater. J.* **2013**, *32*, 115–121. [[CrossRef](#)] [[PubMed](#)]
12. Shu, T.; Okajima, M.; Shimokawa, K.-I.; Ishii, F. The treatment effect of the burn wound healing by electrolytic-reduction ion water lotion. *Biosci. Trends.* **2010**, *4*, 1–3. [[PubMed](#)]
13. Su, Y.; Komasa, S.; Li, P.; Nishizaki, M.; Chen, L.; Terada, C.; Yoshimine, S.; Nishizaki, H.; Okazaki, J. Synergistic effect of nanotopography and bioactive ions on peri-implant bone response. *Int. J. Nanomed.* **2017**, *12*, 925–934. [[CrossRef](#)] [[PubMed](#)]
14. Roy, M.; Pompella, A.; Kubacki, J.; Szade, J.; Roy, R.A.; Hedzelek, W. Photofunctionalization of titanium: An alternative explanation of its chemical-physical mechanism. *PLoS ONE* **2016**, *11*, e0157481. [[CrossRef](#)] [[PubMed](#)]
15. Uetsuki, K.; Nakai, S.; Shirotsaki, Y.; Hayakawa, S.; Osaka, A. Nucleation and growth of apatite on an anatase layer irradiated with uv light under different environmental conditions. *J. Biomed. Mater. Res. A* **2013**, *101*, 712–719. [[CrossRef](#)] [[PubMed](#)]
16. Ogawa, T. Ultraviolet photofunctionalization of titanium implants. *Int. J. Oral Maxillofac. Implants* **2014**, *29*, e95–e102. [[CrossRef](#)] [[PubMed](#)]
17. Iwasa, F.; Baba, K.; Ogawa, T. Enhanced intracellular signaling pathway in osteoblasts on ultraviolet light-treated hydrophilic titanium. *Biomed. Res.* **2016**, *37*, 1–11. [[CrossRef](#)]
18. Alfarsi, M.A.; Hamlet, S.M.; Ivanovski, S. Titanium surface hydrophilicity modulates the human macrophage inflammatory cytokine response. *J. Biomed. Mater. Res. A* **2014**, *102*, 60–67. [[CrossRef](#)]
19. Kusakawa, Y.; Yoshida, E.; Hayakawa, T. Protein adsorption to titanium and zirconia using a quartz crystal microbalance method. *Biomed. Res. Int.* **2017**, *2017*, 1521593. [[CrossRef](#)]
20. Lee, J.H.; Ogawa, T. The biological aging of titanium implants. *Implant Dent.* **2012**, *21*, 415–421. [[CrossRef](#)]
21. Minamikawa, H.; Ikeda, T.; Att, W.; Hagiwara, Y.; Hirota, M.; Tabuchi, M.; Aita, H.; Park, W.; Ogawa, T. Photofunctionalization increases the bioactivity and osteoconductivity of the titanium alloy ti6al4v. *J. Biomed. Mater. Res. A* **2014**, *102*, 3618–3630. [[CrossRef](#)] [[PubMed](#)]
22. Kuroshima, S.; Kaku, M.; Ishimoto, T.; Sasaki, M.; Nakano, T.; Sawase, T. A paradigm shift for bone quality in dentistry: A literature review. *J. Prosthodont. Res.* **2017**, *61*, 353–362. [[CrossRef](#)] [[PubMed](#)]

23. Kuroshima, S.; Nakano, T.; Ishimoto, T.; Sasaki, M.; Inoue, M.; Yasutake, M.; Sawase, T. Optimally oriented grooves on dental implants improve bone quality around implants under repetitive mechanical loading. *Acta Biomater.* **2017**, *48*, 433–444. [[CrossRef](#)] [[PubMed](#)]
24. Okada, Y.; Abe, N.; Hisamori, N.; Kaneeda, T.; Moriyama, S.; Ohmori, H.; Mizutani, M.; Yanai, H.; Nakashima, Y.; Yokoyama, Y.; et al. Verification of implant surface modification by a novel processing method. *Acta Med. Okayama* **2017**, *71*, 49–57.
25. Trisi, P.; Berardini, M.; Falco, A.; Sandrini, E.; Vulpiani, M.P. A new highly hydrophilic electrochemical implant titanium surface: A histological and biomechanical in vivo study. *Implant Dent.* **2017**, *26*, 429–437. [[CrossRef](#)] [[PubMed](#)]
26. Funato, A.; Yamada, M.; Ogawa, T. Success rate, healing time, and implant stability of photofunctionalized dental implants. *Int. J. Oral Maxillofac. Implants* **2013**, *28*, 1261–1271. [[CrossRef](#)]



© 2019 by the authors. Licensee MDPI, Basel, Switzerland. This article is an open access article distributed under the terms and conditions of the Creative Commons Attribution (CC BY) license (<http://creativecommons.org/licenses/by/4.0/>).